Studies of NO_3 Radical Reactions with Some Atmospheric Organic Compounds at Low Pressures

Edward J. Dlugokencky and Carleton J. Howard*

Aeronomy Laboratory, National Oceanic and Atmospheric Administration, Boulder, Colorado 80303, and Cooperative Institute for Research in Environmental Sciences and Department of Chemistry and Biochemistry, University of Colorado, Boulder, Colorado *(Received: March 11, 1988)*

Rate constants for the reactions of NO_3 with *trans*-2-butene (1), isoprene (2), α-pinene (3), and acetaldehyde (4) have been measured as a function of temperature at low pressures in a fast flow system with LIF detection of the NO_3 reactant and NO_2 product. Rate constants for reaction 1 were found to be independent of pressure from 0.44 to 4.5 Torr, and the Arrhenius plot was curved. The data were fit by the four-parameter equation, $k_1(T = 204-378\ \mathrm{K}) = (1.78 \pm 0.36) \times 10^{-12} \exp[-(530 \pm 100)/T] + (1.28 \pm 0.26) \times 10^{-14} \exp[(570 \pm 110)/T]$ (where all the error limits are the 95% confidence levels including a factor for systematic error, and the units are cm^3 $molecule^{-1}$ s^{-1}). The data for isoprene were fit by a normal Arrhenius equation, $k_2(T = 251-381\ \mathrm{K}) = (3.03 \pm 0.45) \times 10^{-12} \exp[-(450 \pm 70)/T]$. The Arrhenius plots for α-pinene and acetaldehyde were linear, and the fits gave $k_3(T = 261-384\ \mathrm{K}) = (1.19 \pm 0.31) \times 10^{-12} \exp[(490 \pm 70)/T]$ and $k_4(T = 264-374\ \mathrm{K}) = (1.44 \pm 0.18) \times 10^{-12} \exp[(-1860 \pm 300)/T]$. The efficiencies for the conversion of NO_3 to NO_2 were determined for reactions of *trans*-2-butene and isoprene at low pressures and room temperature in He, N_2, and O_2 carrier gases, and at 360 K in 1 Torr of He. The measured yields of NO_2 decreased with increasing size of the organic reactant, with increasing pressure, with decreasing temperature, and with increasing deactivation efficiency of the carrier gas. These observations and the temperature dependencies of the rate constants indicate that reactions 1-3 proceed by way of an addition mechanism. From the analysis used to determine the NO_2 yields, NO_2 fluorescence quenching rate constants were determined for isoprene, $k = (3.5 \pm 1.1) \times 10^{-10}$, and *trans*-2-butene, $k = (3.0 \pm 0.9) \times 10^{-10}$.

Introduction

The oxidation of natural and anthropogenic organic compounds has been recognized as an important atmospheric source of CO and other reactive intermediates such as HO_2 and RO_2[1] which ultimately produce ozone. Many kinetic and mechanistic studies of the oxidation of organics by OH and O_3 have been reported,[2,3] but less is known about reactions with nitrate radical (NO_3) as the oxidizing agent.

The reactions of NO_3 with atmospheric organic compounds can lead to formation of HNO_3,[4] peroxyacyl nitrate (PAN),[5] RO_2,[5,6] and toxic compounds such as dinitrates.[6] Since NO_3 is rapidly photolyzed by sunlight, it is present in appreciable quantities only at night. Reactions of organic compounds with NO_3 can then provide a significant loss process for the organic species at night. Therefore, kinetics and product information about these reactions are important for atmospheric models.

Several groups have made room temperature studies of the kinetics and mechanisms of oxidation by NO_3,[5-16] but little is known about the primary products for reactions of NO_3 with organic compounds. Most of the kinetic measurements are from indirect studies at room temperature and atmospheric pressure, and no studies of the temperature and pressure dependencies of the rate constants or the products have been reported. Using the fast flow system with LIF detection, we are able to detect NO_2 and NO_3 with excellent sensitivity and to study reactions as functions of temperaure and pressure in the low-pressure region. We report here the results of studies of NO_3 reactions with the four species: *trans*-2-butene (reaction 1), isoprene (2), α-pinene (3), and CH_3CHO (4). A comparison of our results with the earlier studies done at higher pressures will serve as a test of the applicability of our work to pressures as high as 1 atm.

Experimental Section

The flow tube reactor with laser-induced fluorescence (LIF) detection of NO_3 and NO_2 has been described in detail,[17] so only a brief description is given here.

Temperature control of a 2.54 or a 4.13 cm i.d. Pyrex flow tube was achieved by circulating either silicone oil ($T > 298$ K) or ethanol ($T < 298$ K) from a thermoregulated reservoir through a condenser-like jacket surrounding the reaction zone.

The inside surfaces of the reactor were coated with a halocarbon wax to minimize wall effects. The loss of NO_3 on the halocarbon wax coated reactor walls was small, $k_w \leq 1\ s^{-1}$, at all temperatures. We further tested for wall effects in the reaction of NO_3 with α-pinene at room temperature by changing the surface area to volume ratio, i.e., the diameter of the flow reactor by a factor of 1.6. Curved decay plots were observed for the NO_3 reactions with isoprene and α-pinene at temperatures ≤ 250 K. This was taken to be evidence of wall effects; therefore data for these two reactants taken below 250 K were rejected.

Nitrate radicals were produced in a source reactor by thermal decomposition of N_2O_5 at $\simeq 400$ K and $\simeq 3$ Torr pressure

$$N_2O_5 + He \rightarrow NO_3 + NO_2 + He \qquad (5)$$

where $k_5 \approx 50\ s^{-1}$.[18]

* Author to whom correspondence should be addressed at NOAA R/E/Al-2, 325 Broadway, Boulder, CO 80303.

(1) Zimmerman, P. R.; Chatfield, R. B.; Fishman, J.; Crutzen, P. J.; Hanst, P. L. *Geophys Res. Lett.* **1978**, *5*, 679.
(2) Atkinson, R. *Chem. Rev.* **1986**, *86*, 69.
(3) Atkinson, R.; Lloyd, A. C. *J. Phys. Chem. Ref. Data* **1984**, *13*, 315.
(4) Atkinson, R.; Plum, C. N.; Carter, W. P. L.; Winer, A. M.; Pitts, J. N. Jr. *J. Phys. Chem.* **1984**, *88*, 2361.
(5) Cantrell, C. A.; Davidson, J. A.; Busarow, K. L.; Calvert, J. G. *J. Geophys. Res.* **1986**, *91*, *5347*.
(6) Bandow, H.; Okuda, M.; Akimoto, H. *J. Phys. Chem.* **1980**, *84*, 3604.
(7) Atkinson, R.; Aschmann, S. A.; Winer, A. M.; Carter, W. P. L. *Environ. Sci. Technol.* **1985**, *19*, 87.
(8) Atkinson, R.; Plum, C. N.; Carter, W. P. L.; Winer, A. M.; Pitts, J. N. Jr. *J. Phys. Chem.* **1984**, *88*, 1210.
(9) Atkinson, R.; Aschmann, S. A.; Winer, A. M.; Pitts, J. N. Jr. *Environ. Sci. Technol.* **1984**, *18*, 370.
(10) Atkinson, R.; Carter, W. P. L.; Plum, C. N.; Winer, A. M.; Pitts, J. N. Jr. *Int. J. Chem. Kinet.* **1984**, *16*, 887.
(11) Atkinson, R.; Plum, C. N.; Carter, W. P. L.; Winer, A. M.; Pitts, J. N. Jr. *J. Phys. Chem.* **1984**, *88*, 2361.
(12) Tuazon, E. C.; Sanhueza, E.; Atkinson, R.; Carter, W. P. L.; Winer, A. M.; Pitts, J. N. Jr. *J. Phys. Chem.* **1984**, *88*, 3095.
(13) Japar, S. M.; Niki, H. *J. Phys. Chem.* **1975**, *79*, 1629.
(14) Morris, E. D.; Niki, H. *J. Phys. Chem.* **1974**, *78*, 1337.
(15) Hoshino, M.; Ogata, T.; Akimoto, H.; Inoue, G.; Sakamaki, F.; Okuda, M. *Chem. Lett.* **1978**, *1367*.
(16) Ravishankara, A. R.; Mauldin, R. L. III *J. Phys. Chem.* **1985**, *89*, 3144.
(17) Hammer, P. D.; Dlugokencky, E. J.; Howard, C. J. *J. Phys. Chem.* **1986**, *90*, 2491.

0022-3654/89/2093-1091$01.50/0

The NO_3 fluorescence was excited with an Ar^+ laser pumped ($\simeq$6 W) dye laser ($\simeq$0.4 W) which was tuned to the peak of the strong NO_3 absorption feature at 662 nm and then detected by a cooled photomultiplier tube. The NO_2 fluorescence was excited by using the Ar^+ laser (λ = 514 and 488 nm), and its signal was calibrated directly by adding measured flow rates of NO_2. The NO_3 fluorescence signal was calibrated relative to NO_2 by converting NO_3 to NO_2 by the reaction

$$NO + NO_3 \rightarrow 2NO_2 \qquad (6)$$

$$k_6 = 3 \times 10^{-11}\ \text{cm}^3\ \text{molecule}^{-1}\ \text{s}^{-1}\ (\text{ref } 17)$$

in excess NO, ([NO] $\simeq 1 \times 10^{13}$ molecules cm^{-3}). The detection limit was $\simeq 1 \times 10^8$ molecules cm^{-3} for NO_3 and $\simeq 8 \times 10^7$ molecules cm^{-3} for NO_2 with 15-s signal averaging. All kinetic measurements were made under pseudo-first-order conditions ([organic reactant]/[NO_3] > 100) which produced linear plots of ln $I_f(NO_3)$ vs reaction distance, z, i.e., the distance between the tip of the moveable inlet and the detection region. The reaction distance is equivalent to reaction time, $t = z/v$, where v is the average flow velocity. In the kinetic studies, the $[NO_3]_0$ was in the range (0.6–3) $\times 10^{10}$ molecules cm^{-3}. The use of such low radical concentrations precludes the possibility of any significant interference from secondary reactions. The concentrations of organic reactants were calculated from their flow rates, which were determined by measuring the rate of change in pressure in a known volume. *trans*-2-Butene, isoprene, and α-pinene were added to the flow tube through a moveable inlet. An inert carrier gas was added to the flow to prevent reactant condensation in the inlet. For slow reactions, the necessary addition of large reactant flows through the inlet produced a discontinuity in the flow velocity at the addition point. This problem was circumvented for the reaction of NO_3 with acetaldehyde by modifying the experimental arrangement so that NO_3 was added through the moveable inlet, and the acetaldehyde was added to the carrier gas through a fixed port.

The NO_2 product yields were determined by reacting NO_3 to completion (>99.9%) with excess organic reactant and then measuring the product [NO_2]. The large excess organic reactant concentration assured that there was no significant production of NO_2 by secondary reactions (<1%, even if the secondary reaction rate coefficient were as large as 10^{-11} cm^3 $molecule^{-1}$ s^{-1}). Because of the large concentrations of organic compounds necessary to react NO_3 to completion and the large NO_2 fluorescence quenching rate constants for the organics, a Stern–Volmer analysis[19] was used to determine the NO_2 product yields. The Stern–Volmer equation (for $k_f \ll k_q$ and k_M) is

$$\frac{1}{I_f} = \frac{k_q[\text{organic}] + k_M[M]}{k_f I_a}$$

where I_f is the NO_2 fluorescence intensity (s^{-1}), k_q is the NO_2 fluorescence quenching rate constant for the organic (cm^3 $molecule^{-1}$ s^{-1}), k_M is the NO_2 fluorescence quenching rate constant for the bath gas (cm^3 $molecule^{-1}$ s^{-1}), k_f is the NO_2 fluorescence decay rate (s^{-1}), and I_a is the rate of photon absorption by NO_2 (s^{-1}). The NO_2 fluorescence intensity was measured over at least a factor of 5 in [organic], and Stern–Volmer plots (i.e. plots of $1/I_f$ vs [organic]) were made for each set of conditions of T, P, and carrier gas. The inverse of the intercept is $I_f(0)$, the NO_2 fluorescence intensity in the absence of organic quencher. This signal was due to fluorescence from NO_2 produced in the source reactor and NO_2 produced by the reaction of NO_3 with the organic. The [NO_2] from the source reactor was measured and subtracted from the total. The NO_2 yield was calibrated by using the reaction $NO + NO_3 \rightarrow 2NO_2$.

From the slopes ($k_q/k_f I_a$) and intercepts ($k_M[M]/k_f I_a$) of the Stern–Volmer plots, we also estimated the quenching rate constants for isoprene and *trans*-2-butene. Taking the ratio, slope/intercept = $k_q/k_M[M]$, and the carrier gas quenching rate constants, k_M (for M = He, N_2, and O_2), given by Donnelly et al.,[20] the NO_2 fluorescence quenching rate constants were obtained for isoprene and *trans*-2-butene.

The liquid reactants, isoprene (>99.5%), α-pinene (>99%), and acetaldehyde (>99%), were transferred into glass storage flasks under a N_2 atmosphere, and the head space above the liquid was immediately pumped out. *trans*-2-Butene (>99%) was used directly from the gas cylinder. The He (>99.999%) carrier gas was passed through a liquid nitrogen cooled molecular sieve filled trap. The O_2 (>99.97%) and N_2 (>99.999%) carrier gases were used without purification.

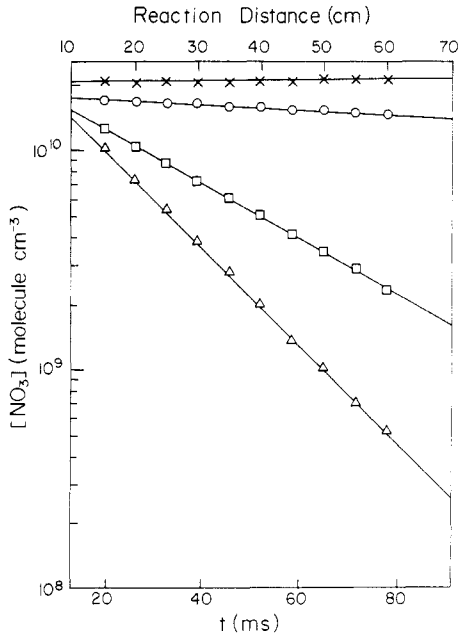

Figure 1. Typical decay plots for NO_3 reaction with *trans*-2-butene. The experimental conditions are T = 297 K; v = 770 cm s^{-1}; P = 1.11 Torr; and [C_4H_8] = 0 (×), 0.67 (○), 7.58 (□), and 13.7 (△), all in 10^{13} molecule cm^{-3}.

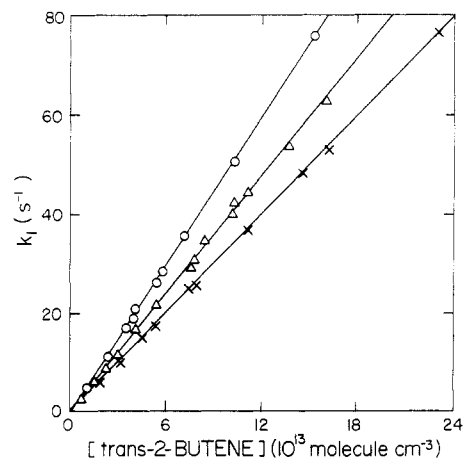

Figure 2. Plot of first-order rate coefficients vs [*trans*-2-butene] for data at 378 K (○), 298 K (△), and 213 K (×). The slopes of the linear fits to each set of data give the second-order rate constants.

Results

For all four reactions, the reaction times were between 24 and 225 ms, and the change in [NO_3] was over factors of $\simeq$1.7–145 for *trans*-2-butene, 2.0–140 for isoprene, 1.3–98 for α-pinene, and 1.1–6.4 for acetaldehyde. Examples of decay plots for the reaction of NO_3 with *trans*-2-butene are shown in Figure 1. The (×)

(18) DeMore, W. B.; Molina, M. J.; Watson, R. T.; Golden, D. M.; Hampson, R. F.; Kurylo, M. J.; Howard, C. J.; Ravishankara, A. R. JPL Publication 85-37, Jet Propulsion Laboratory, Pasadena, CA, 1985.

(19) Okabe, H. *Photochemistry of Small Molecules*; Wiley: New York, 1978; p 62.

(20) Donnelly, V. M.; Keil, D. G.; Kaufman, F. *J. Chem. Phys.* **1979**, *71*, 659.

TABLE I: Summary of Our Rate Coefficient Measurements for Reactions 1–4

T, K	P, Torr	av flow velocity, v, cm s^{-1}	[reactant] range, 10^{13} molecule cm^{-3}	$k \pm 2\sigma$,[b] 10^{-13} cm^3 molecule^{-1} s^{-1}
		trans-2-Butene		
204	1.0	340–500	1.54–12.6	3.46 ± 0.08
206	1.1	200–500	0.84–10.5	3.43 ± 0.11
213	1.1	320–490	1.70–23.3	3.31 ± 0.03
223	1.1	310–530	1.43–18.0	3.27 ± 0.04
243	1.1	350–540	0.69–9.13	3.35 ± 0.07
267	1.1	410–640	1.47–16.6	3.55 ± 0.04
298	0.44–4.5	330–770	0.84–16.0	3.96 ± 0.06
337	1.1	520–750	1.10–11.6	4.37 ± 0.09
378	1.1	470–720	1.06–15.3	4.99 ± 0.05
		$k(T) = (1.78 \pm 0.36) \times 10^{-12} \exp[-(530 \pm 100)/T] + (1.28 \pm 0.26) \times 10^{-14} \exp[(570 \pm 110)/T]$[c]		
		Isoprene		
251	1.1	290–650	0.69–11.4	5.22 ± 0.04
297	1.1	270–780	0.66–9.92	6.52 ± 0.07
347	1.0	370–870	0.68–9.58	8.37 ± 0.14
381	1.1	430–980	0.41–10.1	9.55 ± 0.06
		$k(T) = (3.03 \pm 0.45) \times 10^{-12} \exp[-(450 \pm 70)/T]$[c]		
		α-Pinene		
261[a]	1.1	990–1250	0.086–1.74	78.8 ± 1.6
297[a]	1.0	990–1890	0.072–0.92	62.6 ± 1.4
297	1.0	800–990	0.046–0.94	61.0 ± 3.3
338[a]	1.0	1160–1760	0.16–1.68	51.9 ± 0.8
384[a]	1.0	1300	0.13–1.60	42.4 ± 1.0
		$k(T) = (1.19 \pm 0.31) \times 10^{-12} \exp[(490 \pm 70)/T]$[c]		
		Acetaldehyde		
264	1.3	300–400	42.3–299	$(1.26 \pm 0.04) \times 10^{-2}$
298	1.2	330–460	26.1–260	$(2.74 \pm 0.07) \times 10^{-2}$
332	1.3	350–580	19.1–152	$(5.27 \pm 0.17) \times 10^{-2}$
374	1.1	520–770	25.1–143	$(10.0 \pm 0.20) \times 10^{-2}$
		$k(T) = (1.44 \pm 0.18) \times 10^{-12} \exp[-(1860 \pm 300)/T]$[c]		

[a] Denotes experiments using 2.54 cm i.d. flow tube. All other measurements were made in 4.13 cm i.d. reactor. [b] Errors are 2σ values from the least-squares fits to k^1 vs [reactant] data. [c] Errors are our estimates of the 95% confidence limits.

TABLE II: NO_2 Product Yields[a]

press., Torr	carrier gas: He	O_2	N_2
	Isoprene		
0.5	0.86	0.72	0.74
1.0	0.76, 0.90[b]		
2.0	0.59	0.41	0.43
4.1	0.38		
	trans-2-Butene		
0.5	0.99		
1.0	0.97, 0.95[b]	0.84	
2.0	0.96	0.70	
4.0	0.91		
	α-Pinene		
1.0	0.67		
	Acetaldehyde		
1.0	<0.05		

[a] Uncertainties of yield measurements are estimated to be ±0.1. [b] Yields measured at 360 K, all other data taken at 298 K.

symbols in Figure 1 represent the increase in NO_3 signal as the reactant inlet was moved with [*trans*-2-butene] = 0. This shows that the NO_3 loss on the moveable inlet surface was negligible. Pseudo-first-order rate constants were determined from the slopes of the plots shown in Figure 1. Figure 2 shows plots of the pseudo-first-order rate constants vs [*trans*-2-butene] at different temperatures, and the second-order rate constants are the slopes of least-squares fits to these data. The intercepts determined from the least-squares fits were on the order of 0 ± 0.2 s^{-1}. A summary of results for the reactions of NO_3 with *trans*-2-butene, isoprene, α-pinene, and acetaldehyde is given in Table I. The second-order rate constants, k, are shown for reactions 1–3 in an Arrhenius plot in Figure 3.

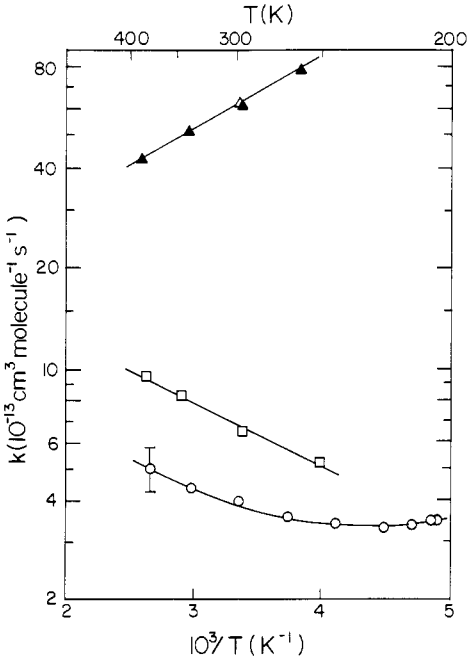

Figure 3. Arrhenius plots for the reactions of NO_3 with α-pinene (△), isoprene (□), and *trans*-2-butene (○). One error bar is shown to illustrate the 95% confidence limit of ±12%. The solid lines are the fits to our data.

The total flow tube pressure for most experiments was ≃1.1 Torr. Some runs for the reaction of NO_3 with *trans*-2-butene were made at room temperature over the pressure range 0.44–4.5 Torr. There was <4% variation in the measured rate constants, and thus no systematic trend in k with P was observed over this pressure range.

TABLE III: NO_2 Fluorescence Quenching Rate Constants

P, Torr	slope/intercept, 10^{-16} cm^3 molecule^{-1}	k_a,[b] 10^{-10} cm^3 molecule^{-1} s^{-1}
	trans-2-Butene	
	He	
0.53	5.30	3.20
1.06	2.69	3.25
2.07	1.38	3.25
4.19	0.64	3.03
1.06[a]	3.02	3.02
	O_2	
1.02	1.43	2.56
2.03	0.70	2.50
		3.0 ± 0.9[c]
	Isoprene	
	He	
0.52	5.61	3.32
1.07	3.09	3.76
2.11	1.58	3.79
4.19	0.96	4.59
1.05[a]	3.28	3.27
	O_2	
0.51	3.24	2.90
2.03	0.92	3.28
	N_2	
0.51	3.35	3.31
2.04	0.90	3.57
		3.5 ± 1.1[c]

[a] Data obtained at 360 K. All other data obtained at 298 K. [b] Our relative rate coefficients are placed on an absolute basis by using the data of Donnelly et al.[20] The error limits are the 95% confidence limits and include the 5% error limits for the rate coefficients reported in Donnelly et al.,[20] and an estimate of our uncertainties. [c] Recommended value.

A summary of the NO_2 product yields is given in Table II. Most of the measurements were made at 298 K. Figure 4 is a plot of $1/I_f$ vs [*trans*-2-butene] at 1.06 Torr and 298 K. The intercept represents $[NO_2] = 6.2 \times 10^{10}$ molecules cm^{-3}, where the $[NO_2]$ from the NO_3 source is 3.3×10^{10} molecules cm^{-3}, and the initial $[NO_3]$ is 3.0×10^{10} molecules cm^{-3}. The data indicate an NO_2 yield of $\simeq 0.97^{+0.03}_{-0.1}$. The smaller upper error limit is the result of an upper limit on the NO_2 yield of unity. A Stern–Volmer analysis was not made for α-pinene because its low vapor pressure restricted the range of obtainable α-pinene flow rates. The yield of NO_2 from the α-pinene reaction was determined in the same way as described in the Experimental Section for *trans*-2-butene and isoprene, except that the NO_2 LIF quenching correction was determined as the ratio of the NO_2 LIF signal with and without the α-pinene present for an added $[NO_2] = 3.3 \times 10^{10}$ molecules cm^{-3}. No NO_2 product was observed for the reaction of NO_3 with acetaldehyde, indicating <5% yield.

The Stern–Volmer analysis used to determine the NO_2 yields was also used to calculate the ratio of NO_2 fluorescence quenching rate constants for organic reactants and carrier gases (k_q/k_M). From the published values for the NO_2 fluorescence quenching rate constants of He, O_2, and N_2 from Donnelly et al.[20] ($k_{He} = (3.51 \pm 0.16) \times 10^{-11}$, $k_{O_2} = (5.42 \pm 0.22) \times 10^{-11}$, and $k_{N_2} = (5.98 \pm 0.28) \times 10^{-11}$, all in units of cm^3 molecule^{-1} s^{-1}), the NO_2 fluorescence quenching rate constants for *trans*-2-butene and isoprene were calculated. These data are summarized in Table III.

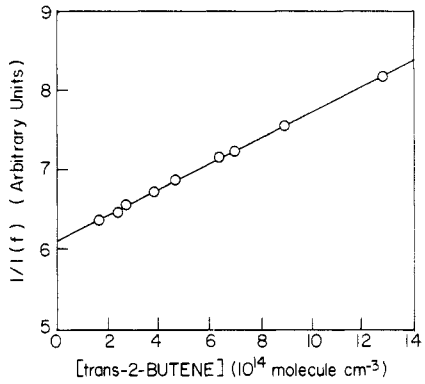

Figure 4. Plot of $1/I_f$ vs [*trans*-2-butene] for Stern–Volmer analysis for the conditions, P = 1.06 Torr and T = 298 K.

All organic reactants were used directly from their storage containers, but α-pinene was also used in a mixture with He (typically $\simeq$3% α-pinene by volume). We found that after allowing the α-pinene mixture to sit in a glass bulb for greater than 1 week, we obtained a second-order rate constant that was ~ 1.7–2.3 times larger than the rate constant obtained by using α-pinene directly from its storage vessel. We did not investigate the cause of this discrepancy, but one possible explanation is that the α-pinene decomposed to give other compounds which were more reactive toward NO_3. For all the data reported here, α-pinene mixtures were used within 2 days of being prepared. In this case, the rate constants obtained with the α-pinene/He mixtures were always within 8% of those obtained by using pure α-pinene.

Discussion

The precision of the kinetic measurements for reactions 1–4, as estimated from a propagation of error analysis, is ±9% at the 95% confidence level.[17] This can be compared with the 2σ limits for the second-order rate constants determined from the slopes of least-squares fits of k^I vs [reactant], which are in the range 1–5% but are typically $\simeq$2%. Although this shows that the precision of the measurements is quite high, neither of these error estimates includes contributions from possible systematic errors such as reaction of NO_3 with impurities or due to wall effects. Including a factor for systematic errors, the uncertainty is estimated at the 95% confidence level as ±12%. The errors in the Arrhenius parameters are our estimates of the 95% confidence limits. For the NO_2 fluorescence quenching rate constants, the measurements made in O_2 are $\simeq$20% smaller than those made in He for both *trans*-2-butene and isoprene. This trend may be due to the small number of measurements made in our study, errors in the rate constants reported by Donnelly et al.,[20] or a combination of both. The overall uncertainties in our quenching rate constant measurements are estimated as ±30% at the 95% confidence level.

The linearity of the decay plots (Figure 1) and the absence of significant intercepts in the plots of k^I vs [organic] (Figure 2) support our conclusion that we are observing homogeneous first-order reaction kinetics. Our studies of the α-pinene reaction

TABLE IV: Room Temperature Rate Constants (k, cm^3 molecule^{-1} s^{-1}) for Reactions 1–4

trans-2-butene (1)	isoprene (2)	α-pinene (3)	acetaldehyde (4)	technique[a]	ref
$(3.96 \pm 0.48) \times 10^{-13}$	$(6.52 \pm 0.78) \times 10^{-13}$	$(6.18 \pm 0.74) \times 10^{-12}$	$(2.74 \pm 0.33) \times 10^{-15}$	FT, LIF	this work
$(3.80 \pm 0.43) \times 10^{-13}$			$(2.41 \pm 0.50) \times 10^{-15}$	SC, I, FTIR	8[b]
	$(5.81 \pm 0.68) \times 10^{-13}$	$(6.1 \pm 1.4) \times 10^{-12}$		SC, I, FTIR	9[b]
			$(1.2 \pm 0.3) \times 10^{-15}$[c]	SC, I, IR A	14
$(1.4 \pm 0.4) \times 10^{-13}$[c]				SC, I, IR A	13
			$(2.1 \pm 0.4) \times 10^{-15}$	SC, I, FTIR	5
$(3.78 \pm 0.41) \times 10^{-13}$				FT, LIF, A	16

[a] FT = flow tube, LIF = laser-induced fluorescence, SC = smog chamber, I = indirect technique, FTIR = Fourier transform infrared detection, A = absorption detection. [b] These rate constants have been corrected as described in ref 12. [c] Discrepancies with these results are discussed in text.

in two flow tubes with different surface area to volume ratios further demonstrates the absence of significant wall effects.

Our results are compared with those of other workers in Table IV. We are in disagreement with the values reported by Niki and co-workers[13,14] who used a 50-L reaction cell and monitored N_2O_5, NO_2, and organic species with long-path IR absorption spectroscopy to study the reactions of organics and NO_3. The equilibrium

$$N_2O_5 + M \leftrightarrow NO_2 + NO_3 + M \quad (5)$$

was employed as a steady-state source of NO_3 radicals. Excess NO_2 was added to the reaction system so that the $[NO_2]$ would be relatively constant over the time period the reaction was monitored. An important contribution of their studies was that, by varying the $[NO_2]$, they proved the reaction was initiated by NO_3 rather than N_2O_5. Rate constants were obtained by fits of their data to the rate equations. The rate constants they obtained with this method were directly related to the equilibrium constant for reaction 5, a value which has been revised significantly since their study. We have used the chemical reaction scheme of Morris and Niki[14] with the currently accepted value for K_5 (K_5(300 K) $= 4.7 \times 10^{10}$ molecules cm^{-3})[18] and our rate constant, k_4, to obtain fits to their data that are consistent with our study.

The rate coefficients for NO_3 reactions with many different organic compounds have been determined by the University of California Riverside group,[7-11] whose studies have included the reactions of NO_3 with alkanes, alkenes, aldehydes, aromatics, and other species. Their experiments were done in a smog chamber interfaced to a FTIR spectrometer with multipass optics. They used two different indirect techniques to obtain rate constants. The first method involved observing the increased rate of decay of N_2O_5 in the presence of the organic reactant, as described above for Niki et al.[13,14] In the second method, the relative decay of two organic compounds was observed in the presence of a steady-state source of NO_3 radicals. This method required that the rate constant for one of the reactions must be known accurately. Their reference rate constants were determined using the first method. The rate constants of Atkinson et al.[8,9] listed in Table IV have been multiplied by a factor of 1.8 as described in ref 12, and these values are in excellent agreement with our work.

Cantrell et al.[5] used a large glass reaction cell equipped with multiple-reflection optics and interfaced to a FTIR spectrometer to study the reaction of NO_3 with CH_3CHO in air at 700 Torr and 299 K. Thermal decomposition of N_2O_5 was used as a source of NO_3. Kinetic data were obtained by determining the rates of product ($HONO_2$ and PAN) formation and reactant (CH_3CHO) loss and then plotting these rates versus $[CH_3CHO][NO_3]$, where the $[NO_3]$ was determined from the equilibrium constant for reaction 5. The second-order rate constant was determined from the slope of this line. Our value for k_4 is in good agreement with that of Cantrell et al.[5]

Direct measurements of the reactions of NO_3 with *trans*-2-butene and isobutene were reported by Ravishankara and Mauldin.[16] They used a halocarbon wax coated flow reactor with laser-induced fluorescence (LIF) and absorption detection of NO_3 to study the reactions at room temperature and from 1 to 4 Torr pressure. Nitrate radicals were produced by the reaction $F + HNO_3 \rightarrow HF + NO_3$ or by thermal decomposition of N_2O_5. We are in excellent agreement with their study of NO_3 + *trans*-2-butene.

Morris and Niki[14] reported NO_2 as the major product for the reaction of NO_3 with CH_3CHCH_2 in O_2 and argon at 1 atm pressure. They also observed an absorption at 1670 cm^{-1} which they tentatively assigned as an organic nitrite. Hoshino et al.[15] and Bandow et al.[6] have used smog chambers with FTIR detection of reactant, product, and intermediate species to study the $C_3H_6/N_2O_5/O_2/N_2$ system. In addition to FTIR detection, Hoshino et al.[15] used gas chromatography to identify products. Both studies determined that the major product of the NO_3 + CH_3CHCH_2 reaction has an absorption at 1670 cm^{-1}, and this product was identified as $CH_3CH(ONO_2)CH_2(ONO_2)$.[15] Acetaldehyde and NO_2 were determined to be minor products, in contrast to the conclusions of Morris and Niki.[14]

Our product analysis data are not applicable to 1 atm pressure, but the results do provide an interesting insight into the NO_3 olefin reaction mechanisms. There are some trends evident in our NO_2 product yield data shown in Table II. (1) As the size or complexity of the alkene is increased at a given temperature and pressure, the yield of NO_2 decreases. (2) The yield of NO_2 from reaction of NO_3 with isoprene in He at 1 Torr increased when the temperature was increased from 298 to 360 K. Since the yield of NO_2 from the *trans*-2-butene reaction at 298 K was already nearly 100%, a significant increase could not occur when the temperature was increased to 360 K. (3) The room temperature yields of NO_2 from the *trans*-2-butene and isoprene reactions decreased as the pressure was increased or when a carrier gas with a greater deactivation efficiency (N_2 or O_2) was used. (4) Although there are changes in the NO_2 yields with pressure for reaction 1, over these same pressure ranges, the rate constant does not change. In fact, our low-pressure measurements for reactions 1–3 agree extremely well with the data obtained at much higher pressures by Atkinson et al.[8,9] This agreement indicates that our low-pressure rate coefficients for these reactions are applicable at 1 atm pressure.

Atkinson et al.[11] have shown that the room temperature rate constants for H-atom abstraction from alkanes by NO_3 are in the range $(4-10) \times 10^{-17}$ cm^3 $molecule^{-1}$ s^{-1}. Our room temperature rate constants for reactions with alkenes (1–3) are $\simeq 10^3$ times larger; therefore these reactions certainly do not proceed by H-atom abstraction. The general observations cited above about these reactions, along with product data from previous studies[6,14,15] and our observed small temperature dependencies, indicate a different mechanism. As originally proposed by Japar and Niki,[13] the evidence indicates that NO_3 initially adds to the alkene π-bond. The excited adduct can react via at least four pathways: (a) it can be stabilized by collisions with the bath gas, (b) it can decompose to NO_2 plus an alkoxy diradical (a pathway which is unlikely because it is $\simeq 19$ kcal mol^{-1} endothermic), (c) it can decompose to NO_2 plus an epoxide, or, (d) it can undergo H-atom migration and decompose to NO_2 and a carbonyl. These pathways are shown below for the reaction of NO_3 with propene.

$$NO_3 + CH_3CH{=}CH_2 \leftrightarrow (CH_3CHCH_2ONO_2)^\dagger \quad (7)$$

$$(CH_3CHCH_2ONO_2)^\dagger + M \xrightarrow{a} CH_3CHCH_2ONO_2 + M$$
$$\Delta H = -20.2 \text{ kcal mol}^{-1}$$

$$(CH_3CHCH_2ONO_2)^\dagger \xrightarrow{b} NO_2 + CH_3CHCH_2O$$
$$\Delta H = 19.0 \text{ kcal mol}^{-1}$$

$$\xrightarrow{c} NO_2 + CH_3\overset{O}{\overset{/\backslash}{CHCH_2}}$$
$$\Delta H = -36.5 \text{ kcal mol}^{-1}$$

$$\xrightarrow{d} NO_2 + CH_3CH_2CHO$$
$$\Delta H = -60.2 \text{ kcal mol}^{-1}$$

The reaction enthalpies have been calculated using the heats of formation and bond energies in Table V. All of the possible product isomeric forms are not shown. In the reactions of OH radicals with alkenes, addition to the terminal carbon is preferred,[2] so NO_3 addition reactions may be expected to behave similarly. Our observation that pathway a becomes more efficient with increased complexity or size of the organic molecule or carrier gas and with decreased temperature suggests that (a) predominates at high pressure and with large molecules. In the atmosphere, the alkyl nitrate radicals formed by this process probably add O_2 to form peroxy radicals as shown by Bandow et al.:[6]

$$CH_3CHCH_2ONO_2 + O_2 + M \rightarrow CH_3CH(O_2)CH_2ONO_2 + M \quad (8)$$

Hoshino et al.[15] have observed epoxide formation (pathway c).

The addition mechanism observed for the NO_3 + olefin reactions is similar to that for O, OH, and O_3 reactions with olefins. These reactions were compared and analyzed in the earlier publications of Japar and Niki[13] and Atkinson et al.[8] In general the

TABLE V: Thermochemical Data for NO_3 + Propene Reaction Mechanism

compound	$\Delta H_f°_{298}$, kcal mol^{-1}	ref
H	52.1	25
NO_2	7.9	25
NO_3	17.3	26
CH_3CHCH_2	4.9	27
	−22.2	27
$CH_3CH_2CH_2ONO_2$	−41.6	27
$CH_3CH_2CH_2OH$	−61.6	27
CH_3CHCH_2OH	−18	25
CH_3CH_2CHO	−45.9	27
$CH_3CHCH_2ONO_2$	2.0	*a*
CH_3CHCH_2O	33.3	*a*
bond	**bond energy, kcal mol^{-1}**	**ref**
$H-CH(CH_3)CH_2OH$	95.7	*b*
$H-CH(CH_3)CH_2ONO_2$	95.7	*b*
$H-CH(CH_3)CH_2O$	95.7	*b*
$H-OCH_2CH_2CH_2$	103.4	28

[a] Estimated from known enthalpies of formation and bond energies. [b] Estimated from compounds with similar bonds.

reaction rate coefficients of O and OH are larger while those of O_3 are smaller than the corresponding NO_3 reactions. A common feature noted for all of the addition reactions is that the reactivity increases as the degree of substitution next to the double bond increases.

The magnitude of the rate coefficients at room temperature indicates a reaction efficiency of about 1 in 10^2–10^3 gas kinetic collisions for the NO_3 + olefin reactions. The measured temperature dependencies unfortunately give little insight into the origin of the low efficiencies, because *trans*-2-butene has a slightly curved Arrhenius plot, while isoprene has a small negative temperature coefficient and α-pinene has a small positive temperature coefficient. We have no satisfactory explanation of these observations. Interestingly all three data sets extrapolate to about the same $T = \infty$ intercept, $A \simeq 2 \times 10^{-12}$ cm^3 molecule^{-1} s^{-1}. Too little is known about the potential energy surfaces for these reactions to gain any useful insight through the application of reaction rate theories. As discussed in connection with our study of the NO + NO_3 reaction,[17] the magnitudes of the rate coefficients are readily matched with reasonable models, but the temperature dependencies are not.

Our inability to observe NO_2 as a product of the reaction with acetaldehyde and the observed positive temperature dependence for reaction 4 are consistent with an abstraction mechanism:

$$NO_3 + CH_3CHO \rightarrow HNO_3 + CH_3CO \qquad \Delta H = -15.4 \text{ kcal mol}^{-1} \tag{4}$$

The acetyl radical undergoes further reactions in air to form PAN and other species as shown by Morris and Niki[14] and Cantrell et al.[5]

The nighttime reactions of NO_3 with organic compounds are important in atmospheric chemistry when they remove significant amounts of reactants or form significant amounts of products such as alkylperoxy radicals, HNO_3, PAN, toxic dinitrates, aldehydes, etc. Atkinson et al.[9] and Winer et al.[21] have calculated atmospheric lifetimes for *trans*-2-butene, isoprene, and α-pinene with respect to their reactions with the atmospheric oxidants O_3, OH, and NO_3 for typical conditions in clean air and moderately polluted air. The lifetimes of the organic species based on reaction with NO_3 are between a couple of minutes and a few hours. These lifetimes are comparable to, or less than, the corresponding lifetimes due to reactions with OH and O_3. This indicates that reactions with NO_3 can provide significant, if not dominant, loss processes for these species.

In conclusion, we have studied the reactions of NO_3 with several organic compounds as a function of temperature and pressure. Because these reactions were studied at pressures significantly lower than tropospheric pressures, it is reasonable to question whether our results apply to tropospheric conditions. For the H-atom abstraction reaction of NO_3 with CH_3CHO, our temperature dependence applies to tropospheric conditions. For the addition reactions between NO_3 and olefins, the product distributions vary with pressure, but the temperature dependence we measure probably applies at atmospheric pressure. It appears that the reaction rate is determined by the rate of formation of the adduct. Essentially all of the excited adducts then yield products, either through collisional stabilization or unimolecular dissociation. Relatively few of the energetic molecules dissociate back to reactants.

Acknowledgment. This work was supported by NOAA as part of the National Acid Precipitation Assessment Program.

Registry No. **1**, 624-64-6; **2**, 78-79-5; **3**, 80-56-8; **4**, 75-07-0; NO_3, 12033-49-7; NO_2, 10102-44-0.

(21) Winer, A. M.; Atkinson, R.; Pitts, J. N. Jr. *Science* **1984**, *224*, 156.
(22) Stockwell, W. R.; Calvert, J. G. *J. Geophys. Res.* **1983**, *88*, 6673.
(23) Cantrell, C. A.; Stockwell, W. R.; Anderson, L. G.; Busarow, K. L.; Perner, D.; Schmeltekopf, A.; Calvert, J. G.; Johnston, H. S. *J. Phys. Chem.* **1985**, *89*, 139.
(24) Johnston, H. S.; Cantrell, C. A.; Calvert, J. G. *J. Geophys. Res.* **1986**, *91*, 5159.
(25) Baulch, D. L.; Cox, R. A.; Hampson, R. F. Jr.; Kerr, J. A.; Troe, J.; Watson, R. T. *J. Phys. Chem. Ref. Data* **1984**, *13*, 1259.
(26) Kircher, C. C.; Margitan, J. J.; Sander, S. P. *J. Phys. Chem.* **1984**, *88*, 4370.
(27) Stull, D. R.; Westrum, E. F. Jr.; Sinke, G. C. *The Chemical Thermodynamics of Organic Compounds*; Wiley: New York, 1969.
(28) McMillen, D. F.; Golden, D. M. *Annu. Rev. Phys. Chem.* **1982**, *33*, 493.